

ORDER VS CHAOS IN NUCLEI

J.P. Blocki¹, J. Skalski¹, I.S. Yatsyshyn², and A.G. M.^{1,2}

¹*Andrzej Soltan Institute for Nuclear Studies, Otwock-Swierk, Poland*

²*Institute for Nuclear Research, Kyiv, Ukraine*

TO THE MEMORY OF WLADEK SWIATECKI

**The 17th Nuclear Physics Workshop “Marie & Pierre Curie”,
Kazimierz 2010**

Plan of talk

1. **INTRODUCTION.** Order and Chaos: Quantum-classical correspondence in the collective dynamics
2. **QUANTUM AND CLASSICAL DYNAMICS**
3. **RELATION TO THE SHELL EFFECTS**
4. **QUANTUM AND CLASSICAL CORRESPONDENCE**
5. **ORDER AND CHAOS THROUGH POINCARÉ SECTIONS**
6. **CONCLUSIONS**

- 1) **WALL FORMULA**, Swiatecki et al. (1977,78),
Koonin, Randrup, Hatch (1977), Abrosimov et al. (1994),
Ivanyuk et al. (1996) **AVERAGING \Rightarrow LOCAL**

- 2) **CLASSICAL \Leftrightarrow QUANTUM COLLECTIVE DYNAMICS,
NON-ADIABATIC NON-LINEAR EFFECTS IN ONE-BODY
DISSIPATION, ORDER vs CHAOS, POINCARÉ SECTIONS
AND LYAPUNOV EXPONENTS**, Swiatecki, Blocki, Skalski et
al. (1995-1999)

- 4) **QUANTUM RESULTS FOR EXCITATION ENERGY**
Magierski, Skalski, Blocki (1997)

- 5) **SHELL AND DEFORMATION EFFECTS IN THE
QUANTUM EXCITATION ENERGY FOR SLOW COLLECTIVE
MOTION AS COMPARED TO THE CLASSICAL PICTURE**

2. QUANTUM AND CLASSICAL DYNAMICS

$$i\hbar \frac{\partial}{\partial t} \psi = \mathcal{H}(t) \psi, \quad \mathcal{H}(t) = \hat{T} + V(r, t)$$

$$V(r, t) = - \frac{V_0}{1 + \exp \{ [r - R(\theta, t)] / a \}}$$

$$R(\theta, t) = R_0 [1 + \alpha_n(t) P_n(\cos\theta) + \alpha_1(t) P_1(\cos\theta)] / \lambda(t),$$

$$\alpha_n(t) = \alpha_{st} + \alpha_n^0 \cos(\omega t), \quad \alpha_n^0 = \alpha \sqrt{(2n+1)/5}$$

$$\psi(t) = \sum_i C_i(t) \phi_i, \quad \Rightarrow \quad \Delta E(t) = E(t) - E(t=0)$$

CLASSICAL WALL FORMULA:

$$\frac{\Delta E_{wf}}{E_0} \propto \left(\tau + \frac{1}{5} \tau^2 \right), \quad \tau = \frac{3}{4} \alpha \eta \left[\omega t - \frac{1}{2} \sin(2\omega t) \right]$$

ADIABATICITY PARAMETER:

$$\eta = \alpha \frac{\omega}{\Omega}, \quad \Omega = \frac{v_F}{R_0}$$

3. RELATION TO THE SHELL EFFECTS

$$H_0\phi_i = \varepsilon_i\phi_i,$$

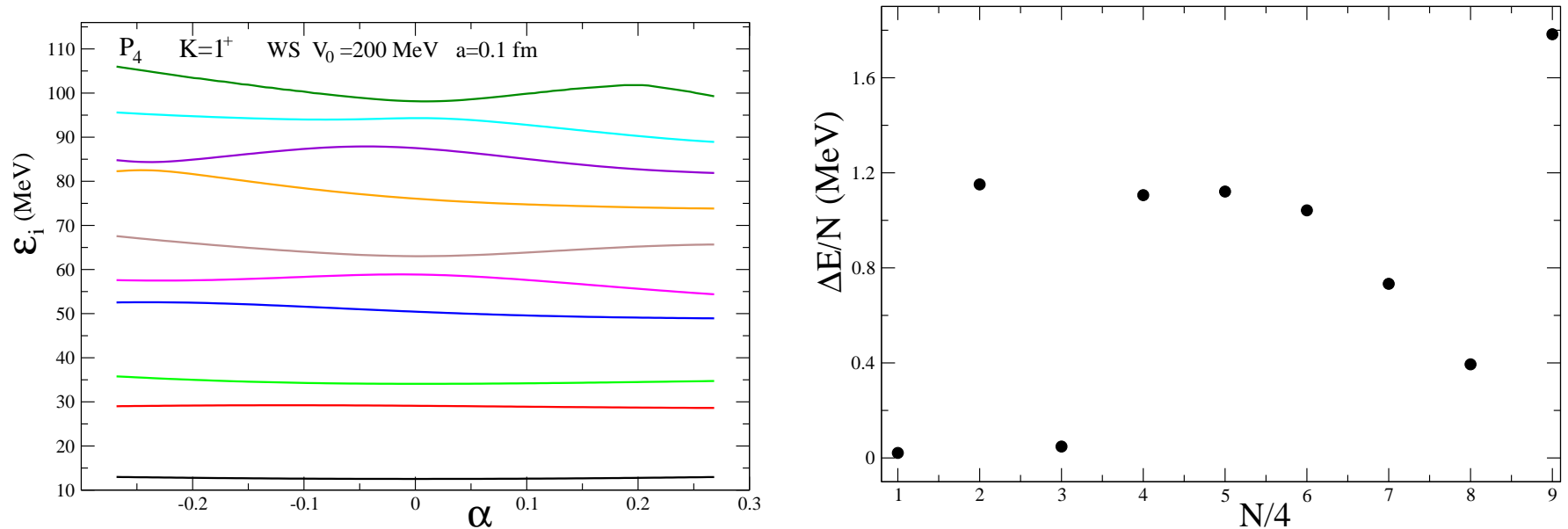


Fig.1. The spectrum of the s.p. levels ε_i as functions of the deformation α for the P_4 shape of the WS potential (left); excitation energy ΔE per particle vs the number of the occupied levels (the particle number N over the degeneracy equal to 4)

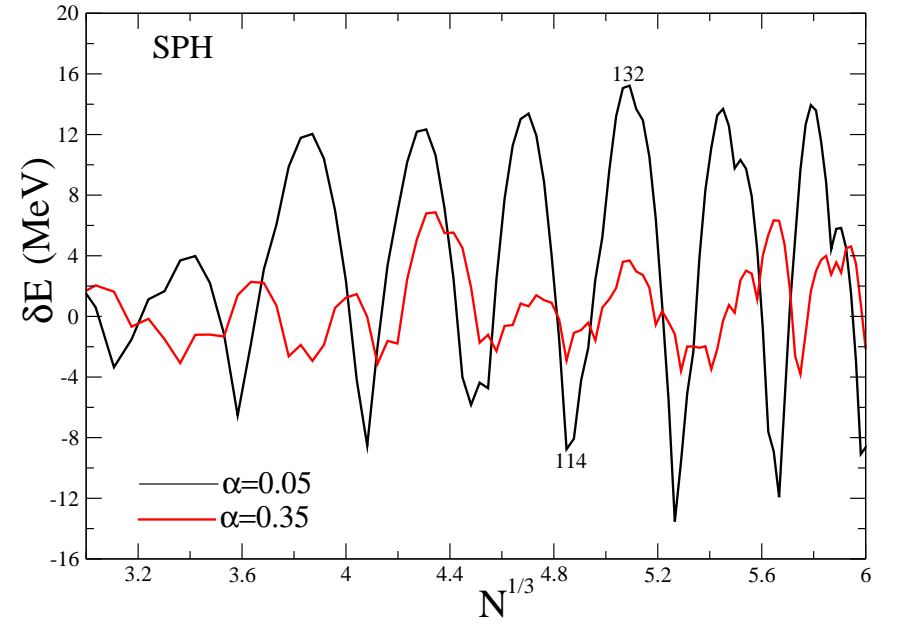
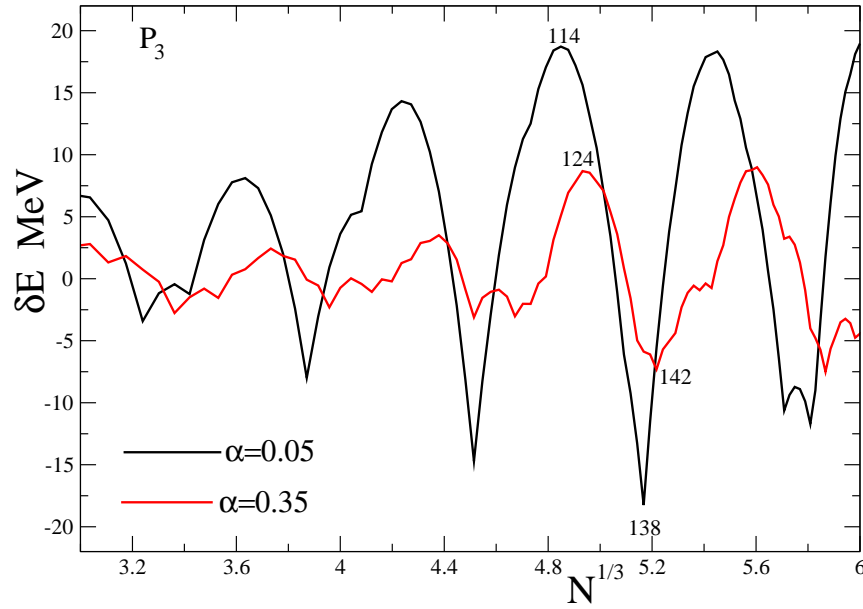


Fig.2. Energy shell corrections $\delta E = E_{s.p.} - \tilde{E}_{s.p.}$ ($E_{s.p.} = \sum_i n_i \varepsilon_i$) as functions of the particle number parameter $N^{1/3}$, $N = \sum_i n_i = \sum_i \tilde{n}_i$, for deformations $\alpha_{st} = 0.05$ and 0.35 for P_3 (left) and those for **spheroidal** (right) shapes, $\delta E \sim \delta g(\varepsilon_F)$, $g(\varepsilon) = \sum_i (\varepsilon - \varepsilon_i)$ is the level density

3. QUANTUM AND CLASSICAL CORRESPONDENCE

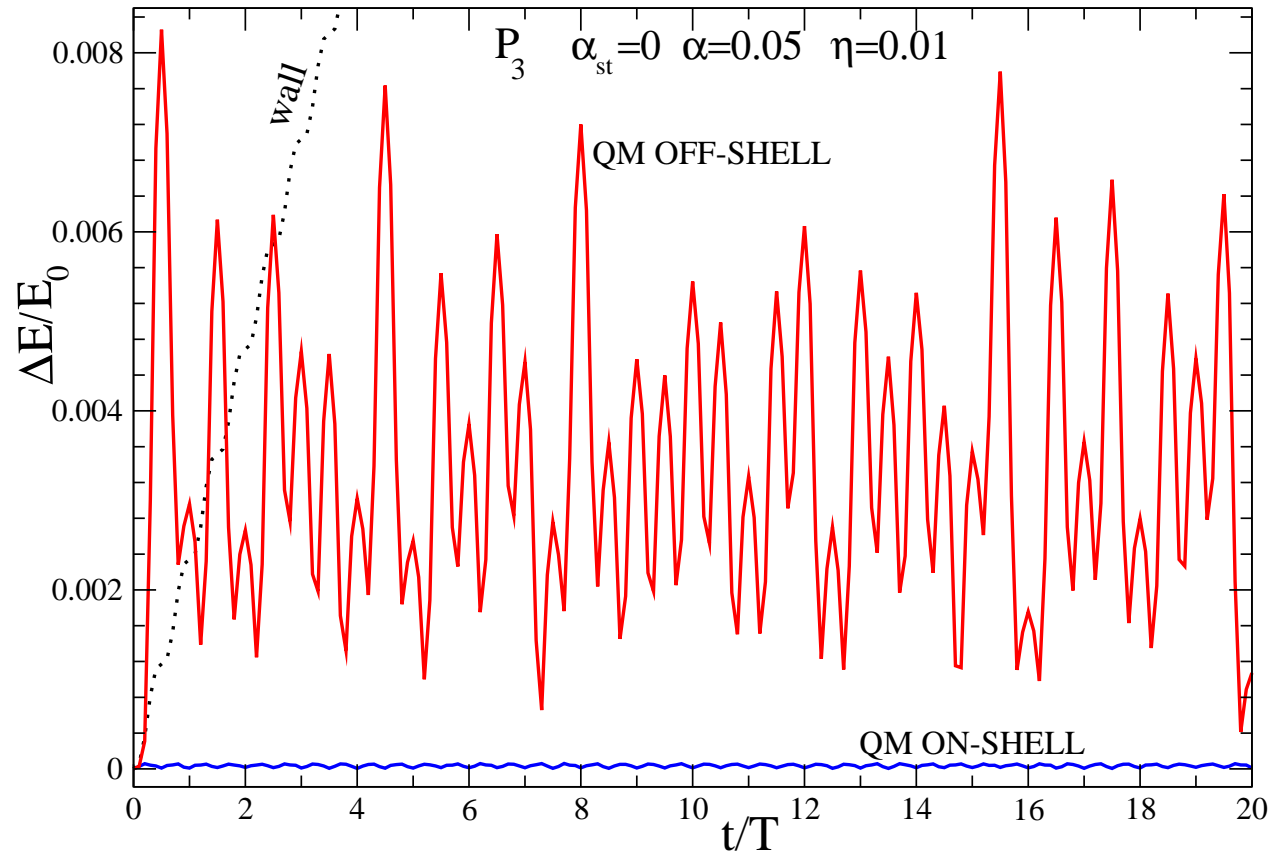


Fig.3. Excitation energy $\Delta E/E_0$ vs the time t in units of the period T for P_3 WS surface shapes; slow ($\omega/\Omega = 0.2$) vibrations of small amplitudes near the spherical shape; QM OFF-SHELL is the quantum results at maximum ($N = 114$) and QM ON-SHELL at minimum ($N = 138$) of δE (or $\delta g(\varepsilon_F)$); averages for QM ON-SHELL and QM OFF-SHELL are $3.6 \cdot 10^{-5}$ and $3.4 \cdot 10^{-3}$

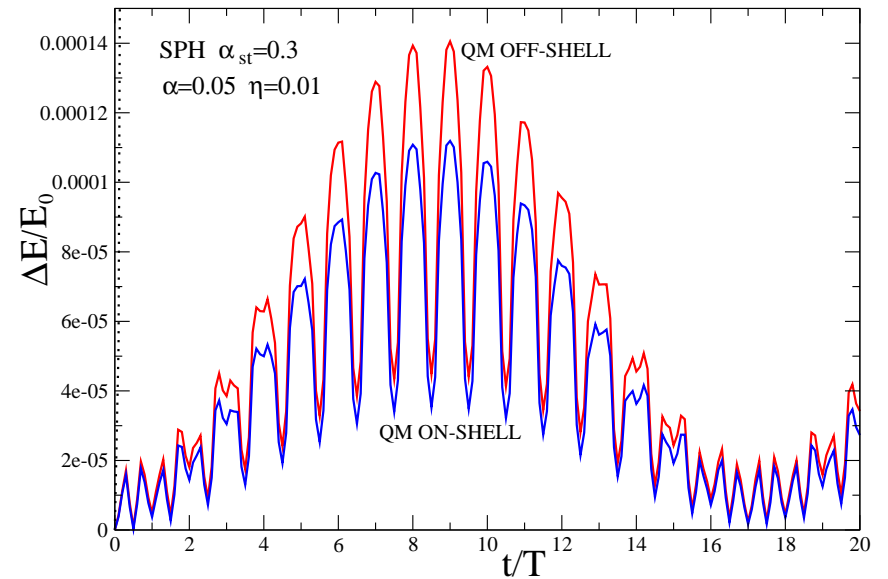
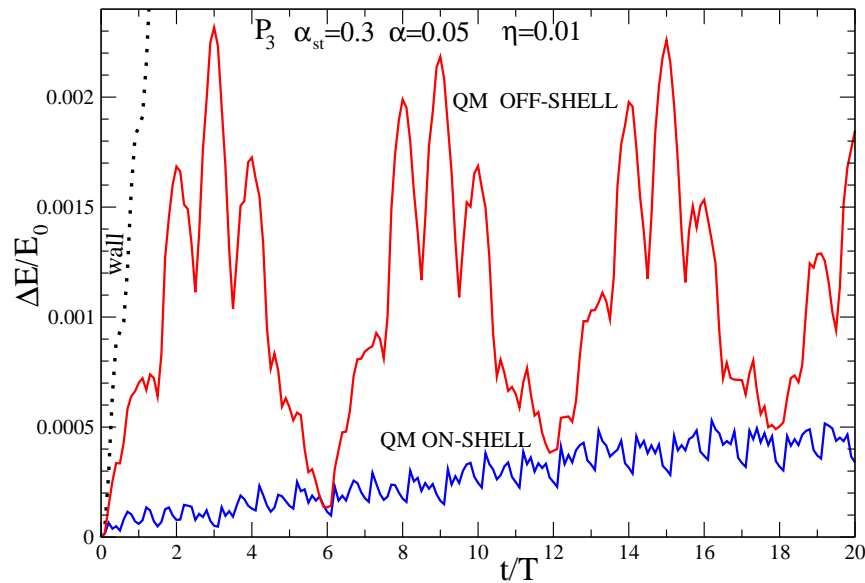


Fig.4. The same as in Fig.3 but for **deformed equilibrium** $\alpha_{st} = 0.3$ of P_3 (left) and **spheroidal** (right) shapes; QM OFF-SHELL is the quantum results at maximum ($N = 124$) and QM ON-SHELL at minimum ($N = 142$) of δE

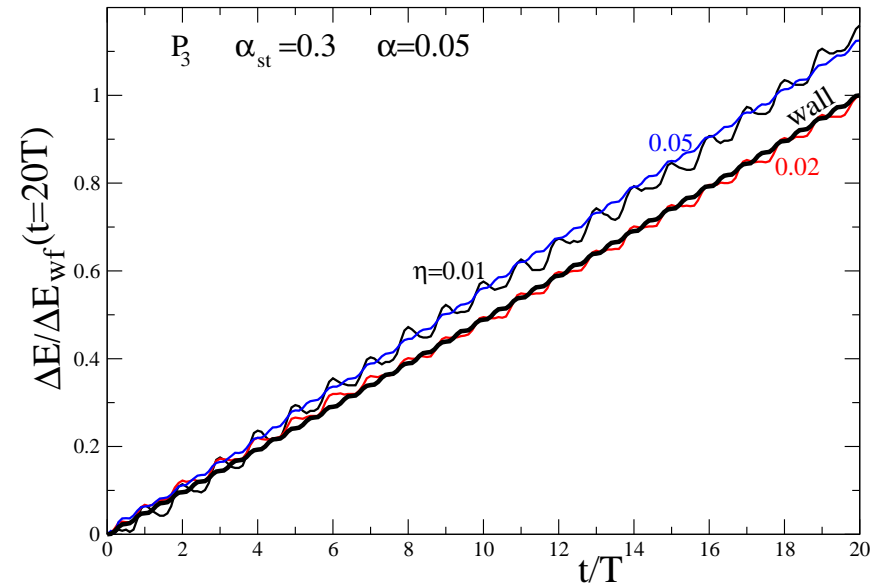
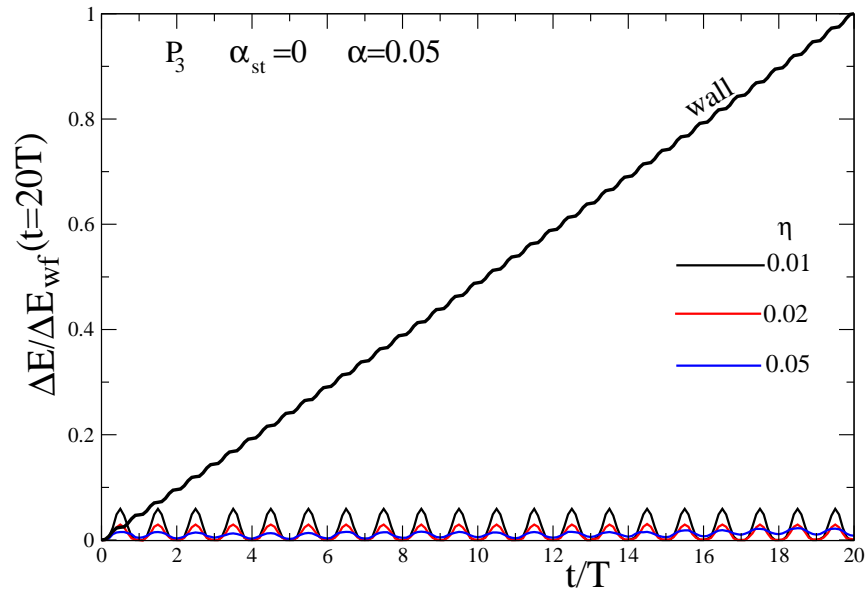


Fig.6. The **classical dynamical excitations** ΔE in units of the wall formula value $\Delta E_{wf}(t = 20T)$ as functions of the time t in units of the period $T = 2\pi\alpha/\eta$ for vibrations near the **spherical** ($\alpha_{st} = 0$, left) and **deformed** ($\alpha_{st} = 0.3$, right) shapes of the cavity

3. ORDER VS CHAOS AND POINCARÉ SECTIONS

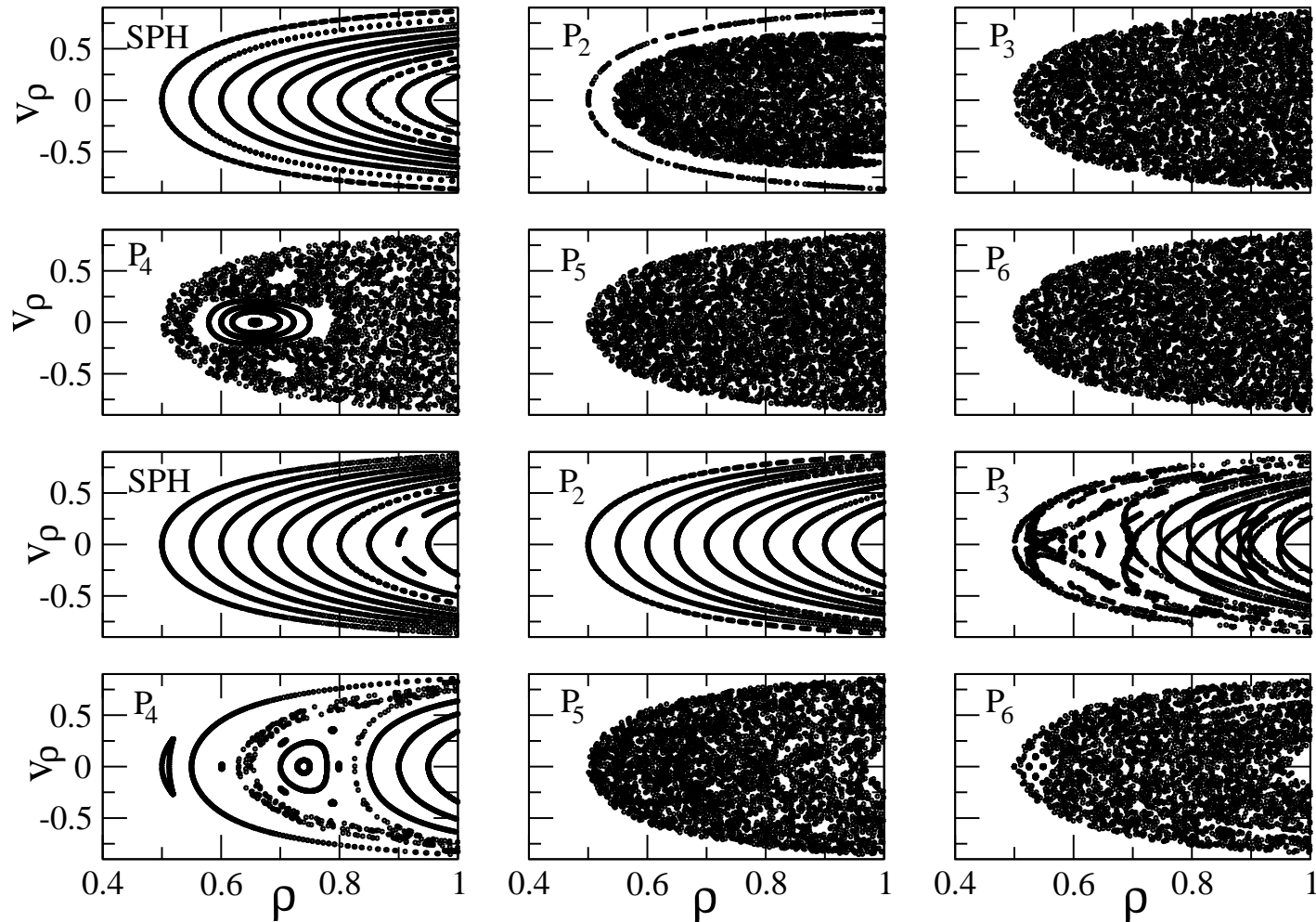


Fig.7. Poincaré sections for six shapes at the **large deformation** $\alpha = 0.4$ (two upper rows) and **small deformation** $\alpha = 0.05$ (two lower rows) for the projections of the angular momentum on the symmetry axis $K = 0.5$ with respect to the maximal value

CONCLUSIONS

- We found the correlations between the **quantum** excitation energies and **shell effects** at **slow collective motion**, the one-body dissipative energies become larger with increasing the **level density** near the Fermi surface
- The **excitation energy** in the **classical** picture as a function of time becomes **closer** to the **wall formula** with **increasing the equilibrium deformation** of the collective vibrations, in contrast to the **quantum** dynamics
- Looking at the Poincare sections, this property can be explained as **increasing of a chaoticity** with the **equilibrium deformation**, the bigger the larger deformation
- **As perspectives**, our **quantum and classical** results might be helpful for better understanding the **dissipative energy** in a **slow and fast** collective dynamics with different **deformed** shapes more **systematically and analytically** for nuclear fission and heavy-ion collision physics

THANKS TO WLADEK SWIATECKI!

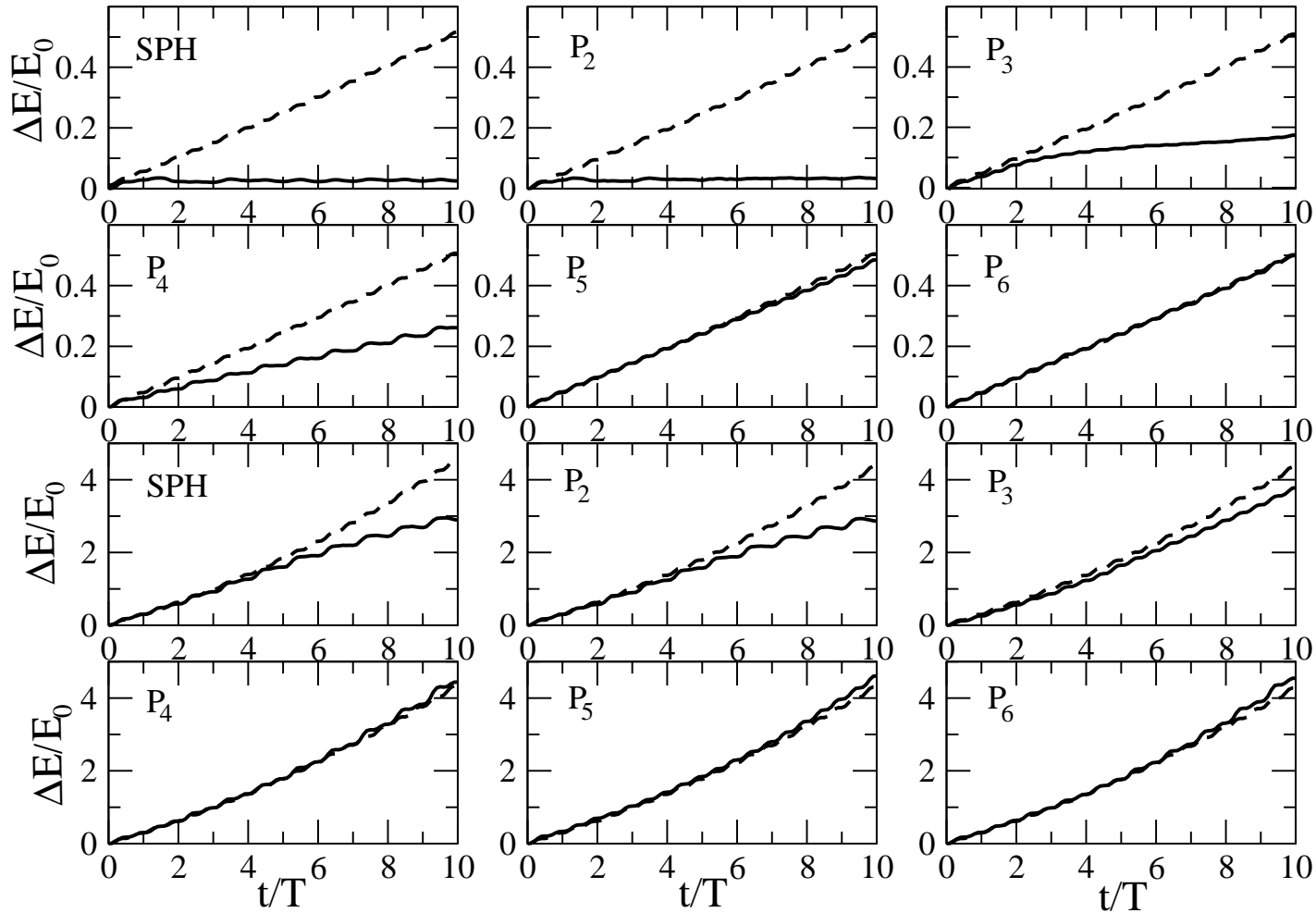


Fig.1. Relative excitation of a gas of particles δE during 10 periods of oscillations around a spherical shape for six shape deformations. The amplitude of vibrations is $\alpha = 0.1$ and the adiabatic parameter $\eta = 0.1$ (upper two rows) and $\eta = 0.6$ (low two rows). Solid lines indicate results of the computer simulations and dashed ones are wall predictions

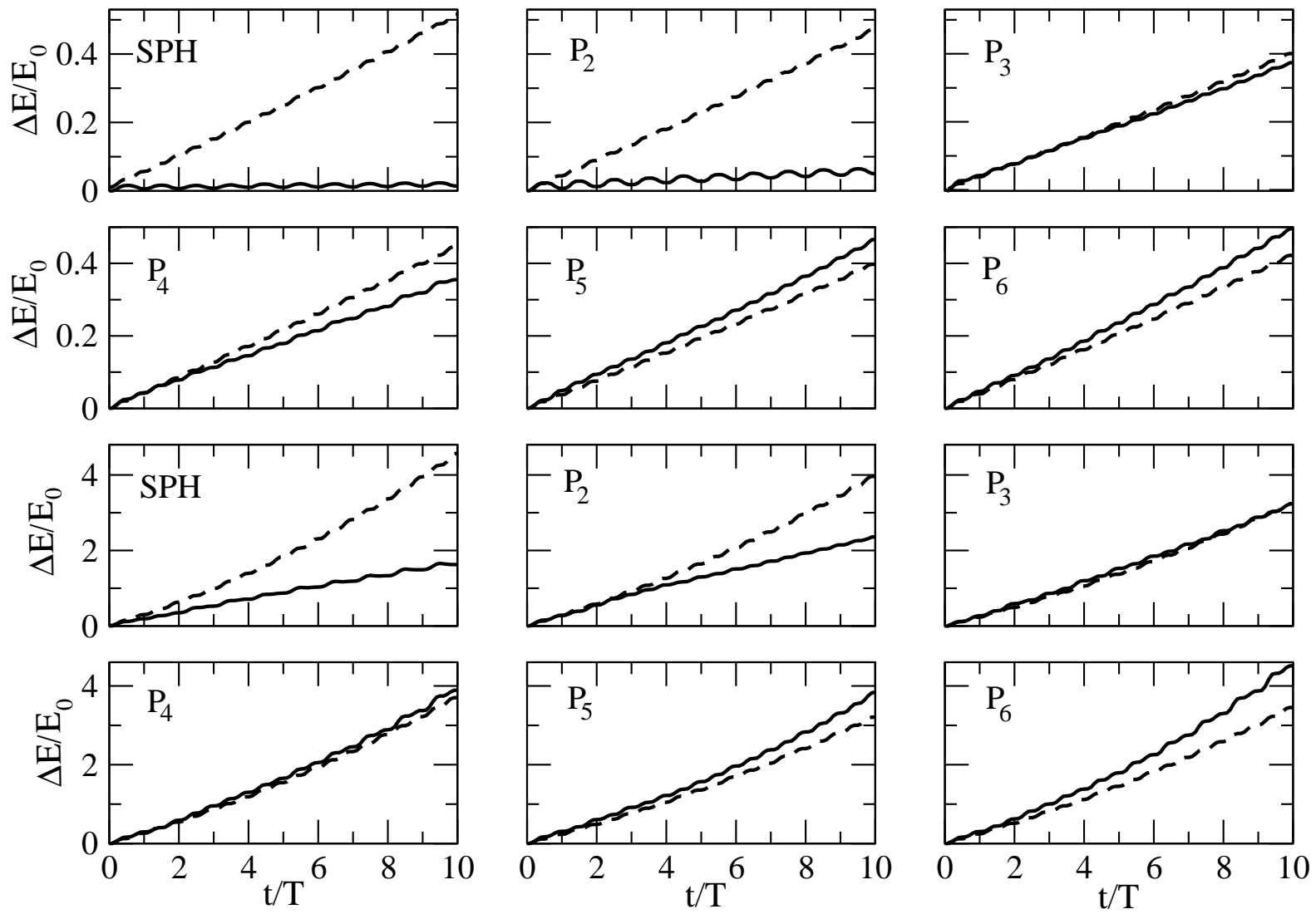


Fig.2. The same as in Fig.1 but for the vibrations around a deformed shape $\alpha = 0.3$

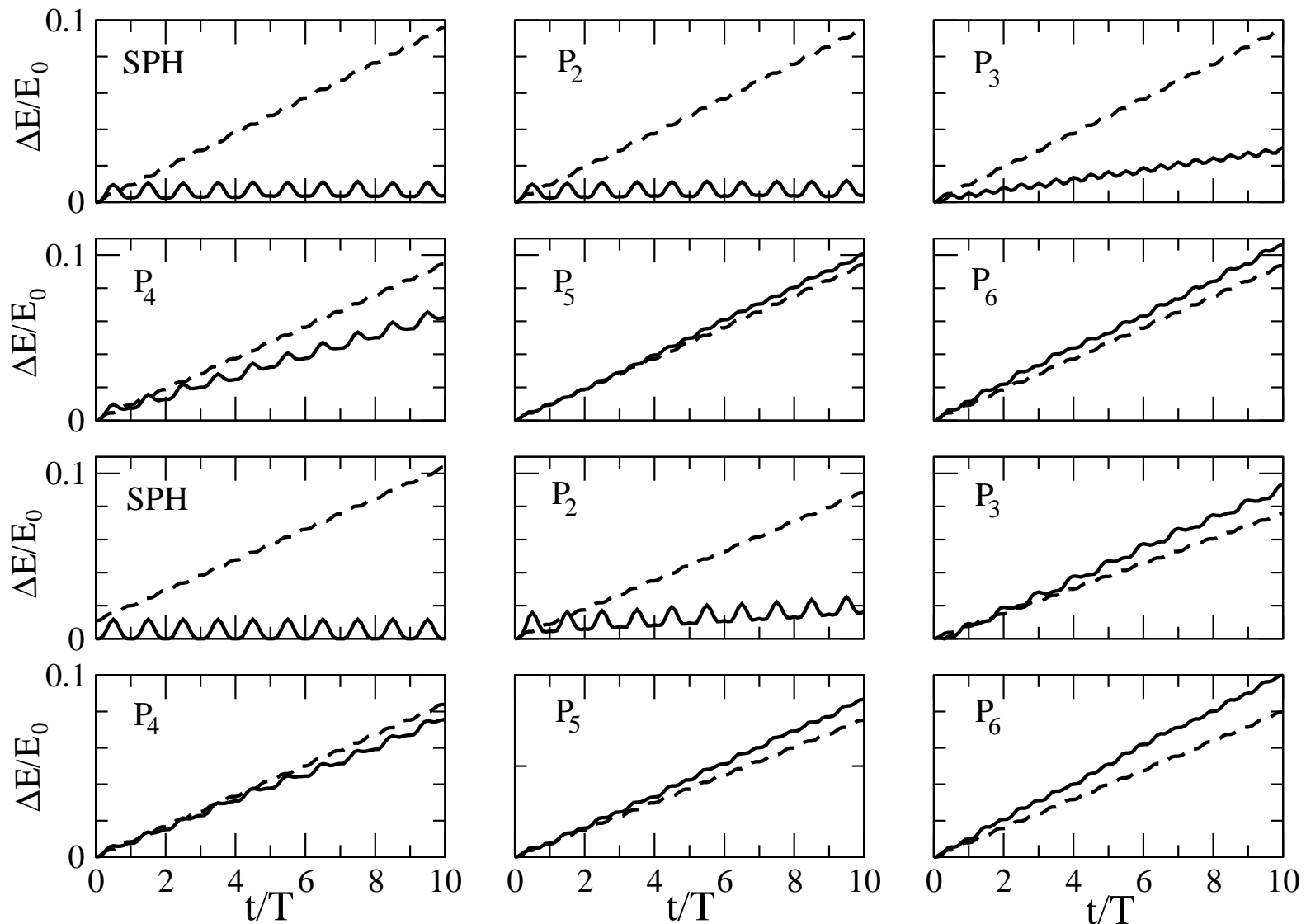


Fig.3. The same as in Figs.1,2 but around a spherical shape (two upper rows) and deformed shape $\alpha_{st} = 0.3$ (two lower rows). The amplitudes of the vibrations is $\alpha = 0.1$ and the adiabaticity parameter $\eta = 0.02$. Solid lines indicate results of the computer simulations and dashed ones are the wall formula predictions

3.

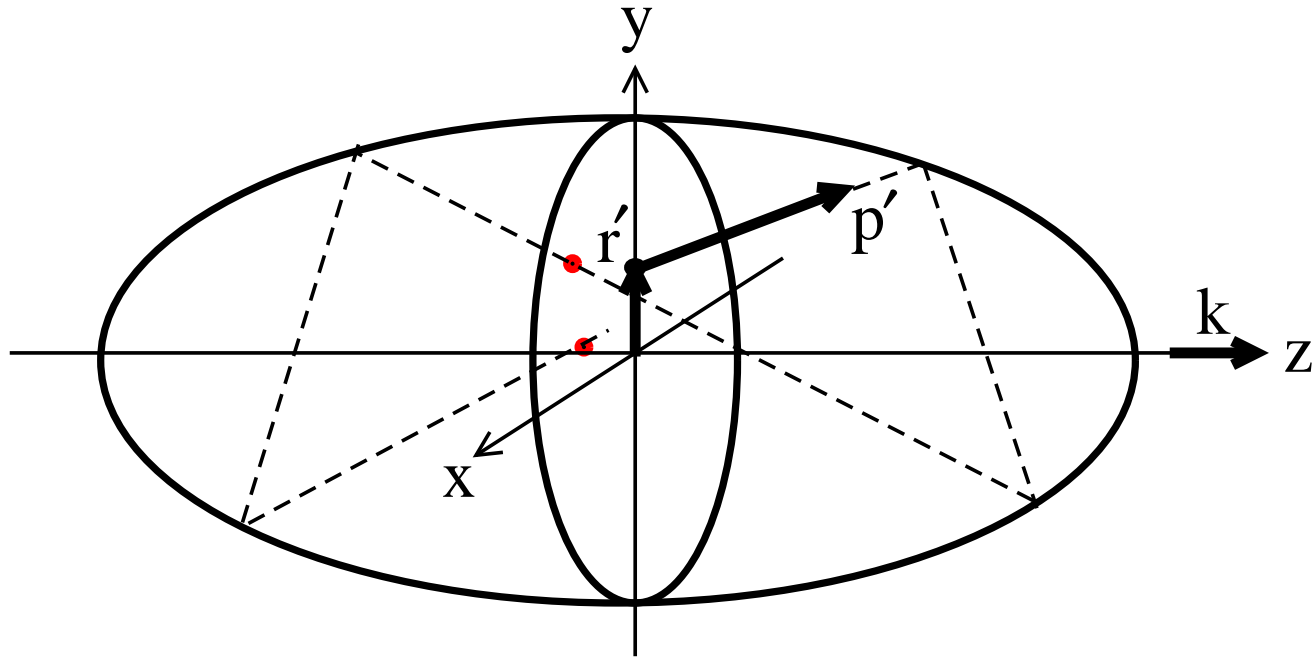


Fig. 4. Poincare section, $\mathbf{K} = (\mathbf{r}' \times \mathbf{p}') \cdot \mathbf{k}$

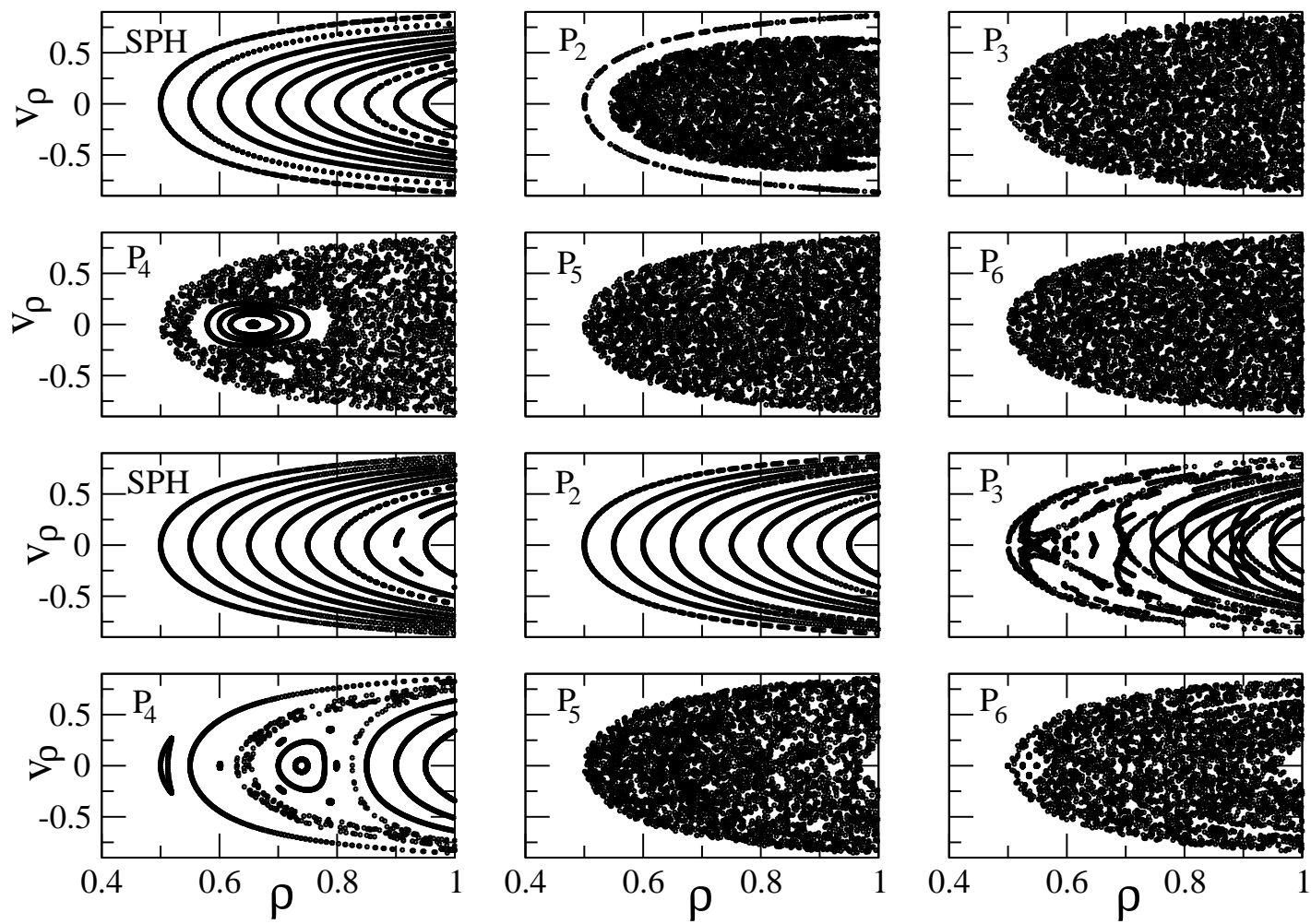


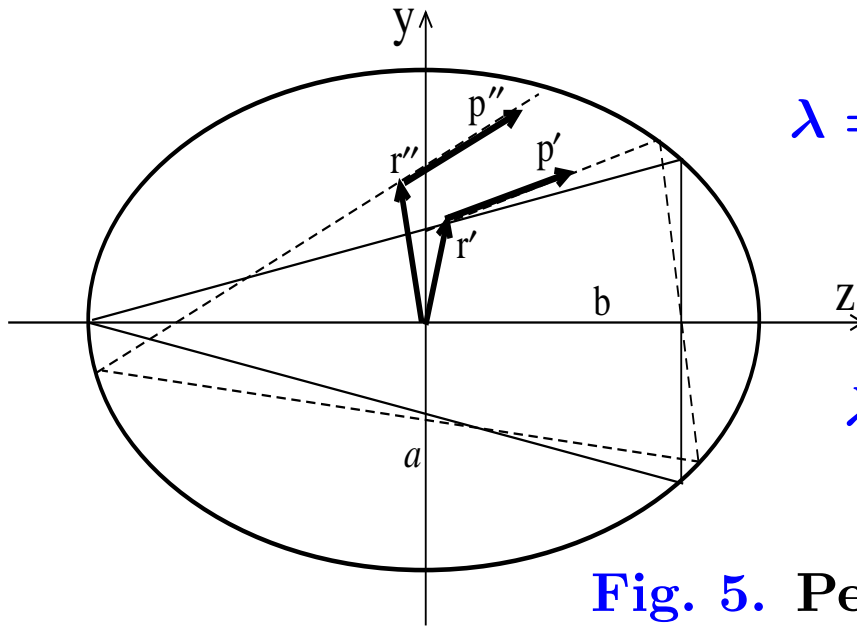
Fig.4. Poincare sections for six shapes at the deformation $\alpha = 0.05$ (two lower rows) and deformation $\alpha = 0.4$ (two upper rows) for the projections of the angular momentum on the symmetry axis $K = 0.5$ with respect to the maximal value

LYAPUNOV EXPONENTS: $\lambda(T)$

MONODROMY MATRIX \mathcal{M} (propagator): $\xi'' = \mathcal{M}(T)\xi'$

$$\xi = \{\delta r, \delta p\}, \quad \mathcal{M} = \begin{pmatrix} \mathcal{M}_\perp & \dots \\ \dots & \mathcal{I} \end{pmatrix}, \quad \mathcal{I} = \begin{pmatrix} 1 & 0 \\ 0 & 1 \end{pmatrix}$$

$tr \mathcal{M}(T) = 1 + 1 + a(T) + 1/a(T)$, $a(T) = \exp[\lambda(T)]$ with period T



$\lambda = i\zeta$ stable p.o., $\lambda = \zeta$ unstable p.o.

$\lambda = \pm 1$ parabolic case, ζ is real

Fig. 5. Periodic-orbit trajectory (p.o., solid) and its variation (dashed) in phase space, $\{r', p'\} \rightarrow \{r'', p''\}$

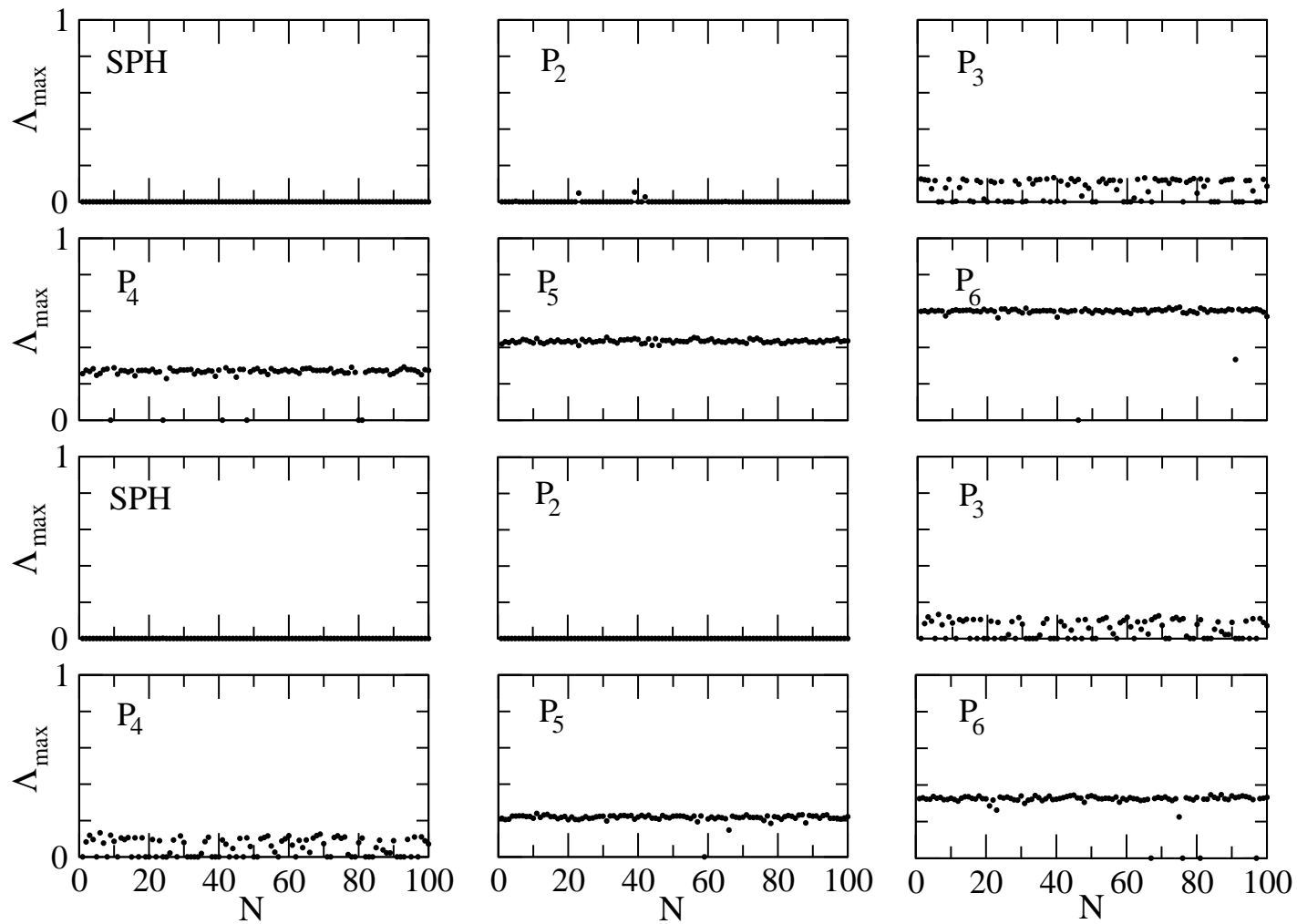


Fig.5. Lyapunov exponents Λ_{max} for six shapes at deformations $\alpha = 0.05$ (lower two rows) and $\alpha = 0.4$ (upper two rows); the projection of the angular momentum on to the symmetry axis $K = 0$

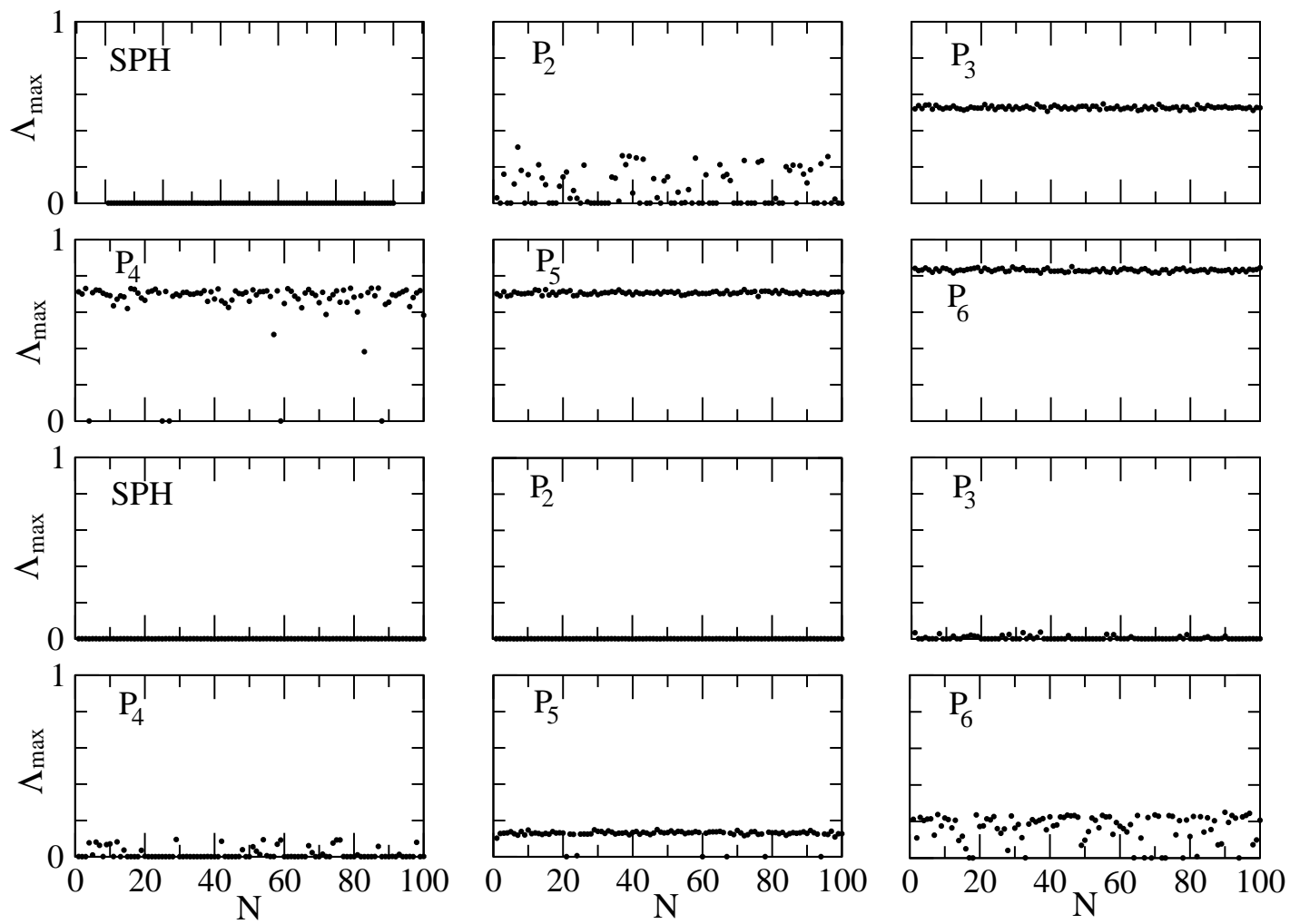


Fig.6. The same as in Fig.5 but for the projection of the angular momentum on to the symmetry axis $K = 0.5$ of the maximal projection